



Object manipulation in immersive virtual environments: Hand Motion tracking technology and snap-to-fit function

Mojtaba Noghabaei^{*}, Kevin Han

Department of Civil, Construction, and Environmental Engineering, North Carolina State University, NC, USA



ARTICLE INFO

Keywords:
 Virtual reality
 Virtual Manipulation.
 Motion Tracking
 Haptic Feedback
 Virtual Assembly

ABSTRACT

There have been recent efforts to use virtual reality and manipulation to train construction workers and inspection. However, there is a lack of research efforts comparing and evaluating virtual manipulation hardware for construction tasks. Moreover, the current practice of virtual manipulation has limited functionality to guide users with the placement of objects in virtual environments. To address these issues, this paper presents 1) a detailed case study that compares three types of manipulation hardware (image-based, infrared-based, and magnetic-based) for construction applications and 2) a snap-to-fit method that improves the VM through solving limitations of the advanced virtual reality interaction metaphors. The latter enhances the placement process for manipulation by comparing two models (e.g., scan and BIM models) for proper placement in assembly scenarios. The case study results show that magnetic-based systems outperform others in construction scenarios. Lastly, the snap-to-fit function was validated in terms of accuracy and time performance.

1. Introduction

Researchers proposed the use of Augmented Reality (AR) and Virtual Reality (VR) to improve communication, efficiency, education, and training in the architecture, engineering, and construction (AEC) industry [1]. AR/VR technologies were utilized by researchers in different industries, such as manufacturing [2,3], retail [4,5], mining [6,7], education [8,9], and healthcare [10] over the past years. Increasing the AR/VR utilization in the AEC industry can potentially address deficiencies, such as lack of real-time and on-site communication [11], lack of communication among stakeholders [12–15], and lack of visualization for engineers and designers [16,17]. AR/VR also exhibited possible applications in domains such as safety training [18], design [19], clash detection [20], compatibility check [21,22], and energy management [23] over the past decade.

Although many researchers studied the visualization aspect of AR/VR, one area that is under-investigated is virtual object manipulation. With recent advances in hardware that allows detection of hand movement while using VR head-mounted display (HMD), this paper focuses on virtual manipulation (VM) in AR/VR environments that can be used for virtual assembly (i.e., assembly of piping systems). Assembly is defined as the process in which two or more objects are coupled and joined together. The current practice for assembly training utilizes two-

dimensional (2D) drawings as the primary visualization means to guide workers. Researchers proposed and experimented with an AR/VR system that was designed for assembly tasks that are normally guided by reference to documentation [24]. The results revealed that the AR/VR system yielded shorter assignment accomplishment periods, fewer assembly faults, and lower task burden [24,25]. The findings through a series of experiments for construction piping assembly revealed that the utilization of AR/VR yielded to a 50% reduction of task completion time and a 50% reduction in assembly errors [25,26]. Findings also indicated that the AR/VR significantly reduced (46%) the rework time and decreased the cost of correcting erroneous assembly by 66%. The results also demonstrated that AR/VR could help improve the workers with lower spatial cognitive abilities the most for the assembly of pipe spools [27,28]. Researchers presented a study that compares the effectiveness of virtual training and physical training for teaching a bimanual assembly task [29]. The results show that the performance of virtually trained participants was promising [29].

Despite these benefits, user interaction with and in AR/VR platforms has been a challenge for the development and full adoption of AR/VR in the AEC industry due to the dynamic nature of the tasks compared to other industries, such as manufacturing [1,30]. Technologies, such as haptic gloves and hand motion tracking, along with AR/VR, are rapidly being developed to overcome the interaction deficiencies [30,31]. The

* Corresponding author.

E-mail addresses: snoghab@ncsu.edu (M. Noghabaei), kevin_han@ncsu.edu (K. Han).

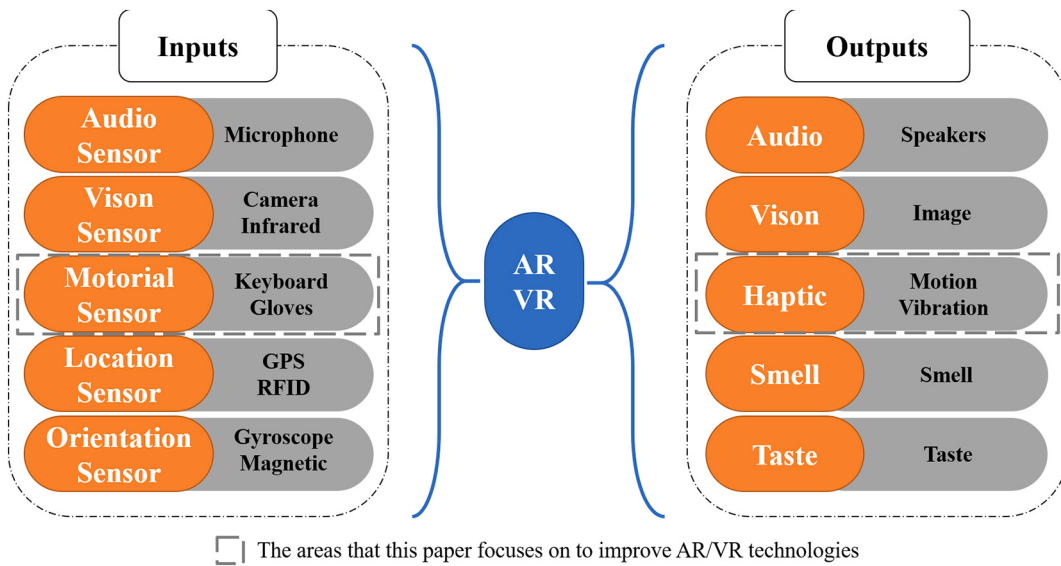


Fig. 1. A taxonomy of AR/VR technologies by their I/O.

interaction in the AR/VR environment using hand motion tracking and haptic technologies are called VM [30]. A VM system consists of hardware and software components. VM hardware comprises of the devices and methods required for tracking body parts (e.g., hand or fingers) and providing haptic feedback in the AR/VR environment. VM software contains the algorithms that perform grabbing, moving, and placing of objects in the AR/VR environment. The development of AR/VR tools and applications for the AEC industry requires considerable research and software development endeavors. The following gaps in the knowledge in the AEC research and practice regarding the VM system are identified (further detailed in Section 2).

Gaps in knowledge:

- 1) Limited research in the AEC domain that utilizes VM systems despite vast potentials for VM technologies.
- 2) Lack of research that compares VM hardware for construction tasks and evaluates the advantages and disadvantages of various VM hardware types, such as image-based, infrared-based, or magnetic-based.
- 3) Limited functionality of VM systems to guide users with the placement of objects in the AR/VR environments [32]. Therefore, researchers suggested the development of a snap-to-fit function to fix the placement deficiencies in VM systems [32].

Limited research efforts on VM applications for the AEC industry indicate the need for structured studies on hardware and software to improve user interaction in AR/VR environments. Therefore, this paper presents advances in knowledge in both VM hardware and software and set the basis for the future development of VM technologies. The specific contributions are as follows:

- 1) Detailed case study through a series of experiments comparing the three types of VM hardware (image-based, infrared-based, and magnetic-based) for AEC applications (Section 3).
- 2) This study focuses on improving the VM through solving limitations of the advanced AR/VR interaction metaphors. This study however, does not focus on improving immersion and realism. The proposed snap-to-fit method improves the placement process for VM, which compares models (e.g., scan and BIM models) for proper placement in assembly scenarios (Section 4). The developed platform is publicly available for the research community so that more functionality can

be added to the platform (please be sure to use the Chrome browser) [33].

In this study, section 3 emphasizes on assessing the state-of-the-art VM hardware through a case study. Whereas section 4 proposes a snap-to-fit method that improves the placement process for VM to address the limitations that are identified in the literature. Therefore, these two sections are not directly dependent. Rather, section 3 aims more on picking the right hardware for VM and section 4 proposes a new placement method that can address limitations of current VM systems. With these contributions, the presented method can be extended to the future development of training programs (e.g., visually guided assembly that a user can follow in a virtual space) and inspection (e.g., compatibility check of a scanned object with other components of a modular component). Also, this VM technology is a cyber-physical system (CPS) that has hardware and software components. Section 3 focuses on its hardware, comparing the state-of-the-art VM hardware through a case study. Section 4 focuses on software through the presented snap-to-fit method that improves the placement process. Together, they make up a CPS system although any of the three hardware can be used for the snap-to-fit function.

2. Background

The Background section examines the existing AR/VR technologies and their applications in the AEC industry as well as other sectors such as manufacturing. Then it identifies gaps for implementing AR/VR and VM in the AEC industry (listed previously as “Gaps in Knowledge”). This section also discusses the potentials of AR/VR with a glimpse over VM technologies and the benefits of adopting AR/VR technologies in the AEC industry.

AR/VR technologies have been rapidly recognized in construction engineering, education, and training programs. AR/VR technologies are the visualization techniques referred to as the pure or partial virtual presence of a user in a virtual environment [34]. AR/VR technologies nowadays are attracting much attention to improve communications in professional work and collaborative spaces [35]. The advantages of using AR/VR in education and training are associated with AR/VR ability to empower users to interact with other users through virtual three-dimensional (3D) environments. AR/VR's visual representation allows a higher level of interaction with virtual elements compared to the conventional education and training methods, such as the utilization

Table 1

An overview of the commercial AR/VR haptic and tracker technologies (* the experimented systems in this paper).

Device	Type	Actuator	Wireless	Hand Tracking	Tactile Feedback	Force Feedback	# Fingers	DoF	Price
*Oculus Quest	Image	Vibrotactile	✓	✓	✓		5	6	\$500
*Motion Leap	Infrared	–		✓			5	6	\$100
Kinect	Infrared	–		✓			5	5	\$100
Gloveone	Glove	Electromagnetic	✓	✓	✓		5	10	\$400
AvatarVR	Glove	Electromagnetic	✓	✓	✓		5	10	\$1250
Senso Glove	Glove	Electromagnetic	✓	✓	✓		5	5	\$600
Cynteract	Glove	Electromagnetic	✓	✓		✓	5	5	–
Maestro	Glove	Electromagnetic	✓	✓	✓	✓	5	5	–
*Noitom Hi5	Glove	Vibrotactile	✓	✓	✓		5	9	\$1000
GoTouchVR	Thimble	Electromagnetic	✓		✓		1	1	–
Tactai Touch	Thimble	–		✓	✓		1	1	–
Woojer	Band	Vibrotactile	✓		✓		–	–	–
CyberGrasp	Exoskeleton	Electromagnetic				✓	5	5	\$50,000
Dexmo	Exoskeleton	Electromagnetic	✓			✓	5	5	\$12,000
HaptX	Exoskeleton	Pneumatic		✓	✓	✓	5	–	–
VRgluv	Exoskeleton	Electromagnetic	✓			✓	5	5	\$600
Sense Glove DK1	Exoskeleton	Electromagnetic	✓				5	5	\$1000
HGlove	Exoskeleton	Electromagnetic				✓	3	9	\$30,000

of stagnant pictures or two dimensional (2D) drawings [36].

An AR/VR framework consists of hardware and software components. The hardware incorporates a processor, display, sensors, and input/output (I/O) devices (a taxonomy of AR/VR I/O hardware [37] is illustrated in Fig. 1). The AR/VR software controls the I/O devices to analyze and respond to user interactions. The software sends signals to the system about the action of the user (e.g., movements of motion tracker gloves) and how the hardware should respond to the user's activities. The software provides appropriate reactions/feedback to the

user through the output devices (e.g., haptic feedback) in real-time.

The AR/VR system could be designed based on the level of immersion or required interactions. The immersion level depends on various combinations of hardware and their configurations. For example, gloves can act as input (e.g., sending hand position) in an AR/VR system and also act as an output for haptic feedback in a scenario when hands collide an object in AR/VR simulations (Fig. 1). In this paper, the authors classified AR/VR systems into low immersion level (low-level) and high immersion level (high-level). Low immersion AR/VR is a system that

Table 2
A summary of AR/VR technologies state of the art applications.

Name	Year	Area of work	Limitations and recommendations	Manipulation device	Key features			
					VR	AR	Manipulation	Haptic
[51]	2020	VR to integrate knowledge and improve safety	VR usage for remote robot control	Virtoba V1	✓	✓		
[52]	2019	VR experiment to study the impact of reinforced learning on fall risk	Lack of accurate motion tracking	Kinect	✓	✓		
[30]	2019	Virtual manipulation for compatibility check	Lack of a snap-to-fit function for object placement in VM	Leap motion	✓	✓		
[50]	2019	A platform for haptic manipulation	The platform requires further accuracy improvement	Leap motion		✓	✓	
[47]	2019	Haptic system for excavator control	Require more sophisticated haptic device	Custom device	✓			
[49]	2019	Human-robot interaction using tracking systems	Required a force feedback system	Leap motion	✓			
[14]	2019	VR for real-time cost estimation	Limited user interactions	–		✓		
[27]	2019	AR Manipulation and training workers	Problems in manipulation	Light scanner		✓	✓	
[27]	2019	VR for assembly training	Needed vibrotactile feedback systems	Oculus Quest	✓	✓		
[19]	2019	VR for design review	VR simulations should be more realistic	HTC	✓	✓		
[53]	2019	VR for design and training	VR software needs to be enhanced for higher adoption in construction	HTC	✓	✓		
[54]	2019	AR for Lean construction and project delivery	Limitations in using the device	Hololens		✓	✓	
[29]	2018	Virtual training for bimanual assembly	Limited operations in Oculus Touch	Oculus Quest	✓		✓	
[38]	2018	AR and VR for off-site and on-site training	Needed a manipulation system	–	✓	✓		
[43]	2018	Robotic construction worker system	Manipulation was not accurate and efficient	Kinect	✓		✓	
[41]	2018	Improving efficiency through enhanced training	Difficulties in engaging users in AR.	–		✓		
[44]	2018	Human-machine interaction for robots	Suggested the use of Haptic Gloves	–				
[35]	2018	VR for constructability analysis	Difficult interaction in 4D VR.	Controller	✓	✓		
[45]	2018	Operator assistant system	Proposed use of haptic gloves for crane control	–		✓		✓
[55]	2017	Training workers using AR in manufacturing	A limited degree of freedom in hand movements	Kinect	✓	✓		
[46]	2017	Excavator remote control using a head tracker	Suggested using haptic gloves for better interaction	–		✓		
[39]	2017	Full body avatar development	Difficulties in action calibration	Motion tracker	✓	✓		
[48]	2016	Introducing the idea of VR manipulation	Occlusion of motion sensor	Leap motion	✓		✓	
[28]	2015	AR/VR training for industrial assembly tasks	Limited user interactions	–	✓	✓		
[32]	2015	Virtual training for assembly	Absence of a snap-to-fit function for VM training	5DT glove	✓	✓	✓	
[25]	2014	Using AR for pipe assembly	AR limitations in object detection	–		✓		
[26]	2014	AR for maintenance instruction	Limited AR interaction	–		✓		
[24]	2013	Assembly training in AR.	Difficulties in interaction using QR code	–		✓		
[40]	2013	Improved interaction with 3D CAD	Difficulties in detecting hand gestures	Kinect	✓	✓		

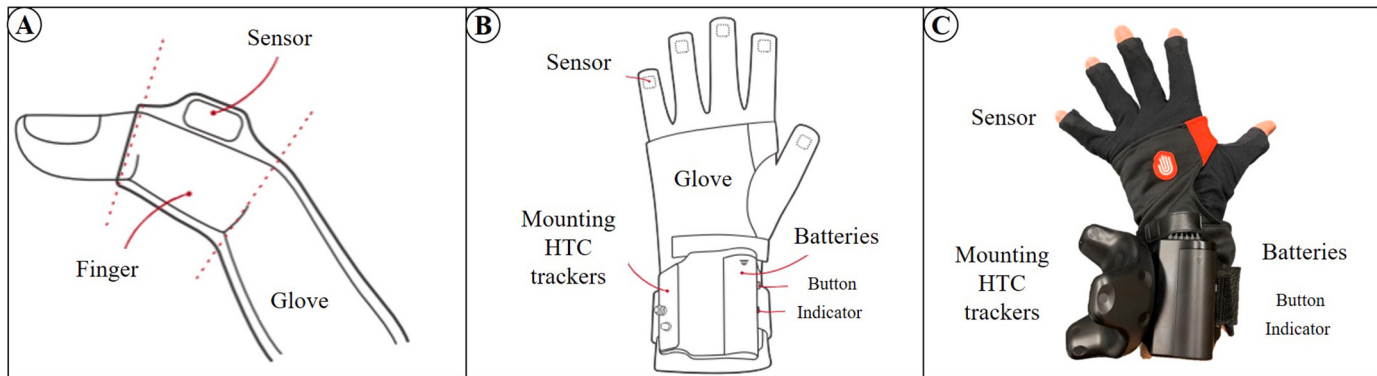


Fig. 2. Noitom Hi5 details; (A) Sensor placement on the finger; (B) Glove placement over the hand; (C) HTC trackers mounted on the glove

does not employ motion trackers or haptic feedback for interaction, while high immersion AR/VR utilizes motion trackers or haptic feedback.

The focus areas of this paper.

A low-level AR/VR system is always limited to certain types of pre-defined interactions through controllers. Utilizing a high-level AR/VR system can enable users to explore and manipulate real and virtual models using new interaction metaphors such as hand motion tracking or haptic feedback systems [38]. Table 1 demonstrates an overview of the commercial AR/VR haptic and tracker technologies sorted by the enabling technology.

Studies indicate that using motion trackers and haptic feedback in AR/VR can significantly improve the AR/VR realism level [39]. Researchers aimed to explore a new generation of interaction metaphors to increase the design review process [40]. They presented a framework that obtains user motion using a combination of video and Kinect (an infrared-based motion detection device developed by Microsoft) and visualizes the CAD/BIM models in AR [40,41]. They evaluated the feasibility and robustness of the interface and identified that this framework requires significant improvements due to the low-accuracy of motion detection [40]. In addition to the low accuracy of motion detection, researchers suggested recruiting haptic devices to improve user interactions in AR/VR training scenarios [42].

Studies investigated virtual bimanual haptic training and classified VM into three sections as grabbing objects, moving objects, and finally placing objects [30]. The researchers separated the object manipulation in an AR/VR environment to three sections of object grabbing, moving, and placing. However, the researchers identified the need for improving the placement operation in VM since the state of the art VM libraries lack such operation and need modifications [30]. The researchers suggested the development of a snap-to-fit function to address the limitations of object placement and enable users to place (snap) an object into a target

area or highlighted mesh [30,32].

Researchers developed a framework for the remote construction worker system to eliminate to increase construction safety [43]. The results identified the gaps in human-machine interfaces for remote-controlled construction robots and suggested the use of haptic gloves for improved user interaction [44]. Researchers also indicated that haptic gloves could boost the remote control of the cranes and excavators [45–47]. Studies suggested using Leap Motion with VR to overcome problems associated with using Kinect and improve user interaction [48]. Researchers ensured high accuracy using Leap Motion [49]. The results show that the Leap Motion can provide users with exceptional interactive experiences [49]. Recent studies advanced Leap Motion through using tactile feedback and concluded that tactile feedback could significantly improve user interaction in the domain of remote surgery [50].

Table 2 depicts a summary of the background section and highlights the main limitations and recommendations of the investigated studies.

3. Comparison of state-of-the-art VM technologies

As discussed in the Background section, AEC researchers did not fully adopt haptic gloves and hand motion trackers [1,30,56]. A detailed comparison of VM systems is not available for the AEC community. To the best of the authors' knowledge, haptic gloves were not adopted in any construction research paper. Therefore, before going into the development of the snap-to-fit function, this section compares a state-of-the-art commercial and research level haptic glove and two different types of hand motion tracker devices for VM tasks. This case study compares the tracking and haptic feedback accuracy of the three common setups to find the optimal setup for the AEC industry and research.



Fig. 3. Leap Motion overview; (A) Leap Motion hardware; (B) Connecting Leap Motion to HTC Vive



Fig. 4. Camera placement on the Oculus Quest HMD.

3.1. VM hardware

Three major VR motion trackers were selected for comparison in this section, and the technical details, accuracy, and performance of these devices were compared through a series of observations while manipulating standard construction objects by typical gestures.

- 1) Noitom Hi5 was selected as the state-of-the-art commercial haptic glove, which is a magnetic-based motion tracker [57]. **Fig. 2** shows an overview of the glove. **Fig. 2(A)** shows sensor placement over the fingers. **Fig. 2(B)** and **(C)** show the essential parts of the gloves, such as the HTC tracker position over the gloves.
- 2) Leap Motion was selected as the conventional infrared-based motion tracker first introduced in 2012 (infrared depth-sensing using a stereo infrared camera) [58]. **Fig. 3(A)** shows the placement of infrared cameras and emitters over the Leap Motion. **Fig. 3(B)** indicates the arrangement of the Leap Motion over a VR HMD.

3) Oculus Quest was selected as an image-based commercial level VR system that has integrated hand motion tracking technology using four peripheral cameras. **Fig. 4** shows the placement of peripheral cameras over the VR HMD.

The first two VM systems (Noitom Hi5 and Leap Motion) were tested using HTC Vive business edition, while the third VM system uses a different VR HMD (Oculus Quest). The two VR HMDs have different hardware; therefore, the graphical and visual capabilities such as field of view and resolution are different. The visual and graphical capabilities of these HMDs were not investigated as this comparison is not within the scope of this study since the focus of this study is on comparing VM hardware for construction tasks and evaluating VM hardware.

3.2. Case study

Four commonly used construction tools were selected to compare the manipulation systems for dealing with different grabbing scenarios (see **Fig. 5**). These tools were chosen in a way to cover various dimensions from small to large. Lastly, these four tools were selected for one hand and two hand manipulation scenarios. For instance, tool D in **Fig. 5** requires two-hand manipulation. The gestures in this section were selected based on the commonly available gestures provided by three VM systems introduced in this section (Oculus, Noitom, and Leap Motion). Also, the objects were selected arbitrarily based on commonly used construction tools of various sizes, from small to large.

In addition to the four tools, four one-handed and two-handed main gestures were defined for grabbing scenarios, not necessarily for operating the four tools but grabbing and picking in general. **Fig. 6** shows the gestures used in this section. In this case study, a computer with an Intel Core i7-6700K, 64 GB of RAM, and Nvidia GTX 1080 was used.

3.3. Findings

Table 3 summarizes the pros and cons of manipulating each object with the three manipulation system. This section's overall findings

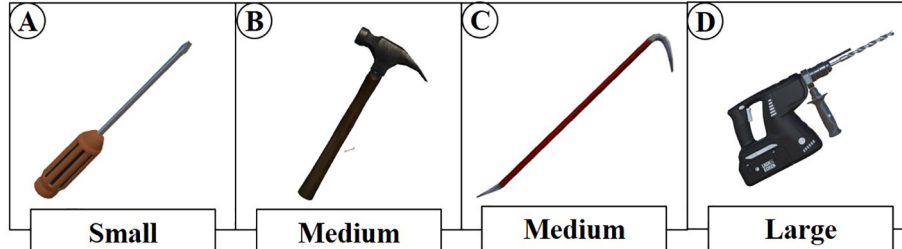


Fig. 5. Objects for manipulation scenarios based on the relative size; (A) Screwdriver; (B) Claw hammer; (C) Crowbar; (D) Power drill.

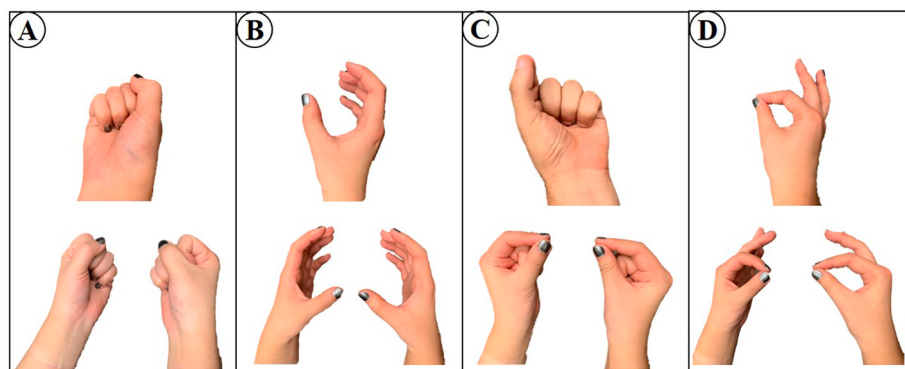


Fig. 6. Defined gestures for grabbing the objects.

Table 3
Comparison of manipulation systems.

Objects		Manipulation Systems	
Screwdriver	Pros	Noitom Hi5 (Magnetic-Based)	Oculus Quest (Image-Based)
	Cons	<ul style="list-style-type: none"> Strong tracking in gesture C and D Calibration difficulties 	<ul style="list-style-type: none"> Strong tracking in fine movements in gesture C Self-occlusion of hands
Claw hammer	Pros	<ul style="list-style-type: none"> Strong tracking in all four gestures Poor performance in the presence of extrinsic magnetic fields 	<ul style="list-style-type: none"> Strong tracking Self-occlusion of hands
	Cons	<ul style="list-style-type: none"> Calibration difficulties 	<ul style="list-style-type: none"> Extremely noisy, especially in gesture type A Strong tracking in gesture D Self-occlusion of hands in gesture A and B
Crowbar	Pros	<ul style="list-style-type: none"> Strong tracking in all gestures Calibration difficulties 	<ul style="list-style-type: none"> Strong tracking Self-occlusion of hands
	Cons	<ul style="list-style-type: none"> Strong tracking in bimanual manipulations Calibration difficulties 	<ul style="list-style-type: none"> Strong tracking in gesture D Noisy performance Excellent performance with two hands in gesture B Bimanual manipulation is not working properly
Overall	Pros	<ul style="list-style-type: none"> Tracks hands in any position without limitation Gloves working only with HTC Vive as Hi5 requires Vive trackers Poor performance in the presence of extrinsic magnetic fields Limited API 	<ul style="list-style-type: none"> Tracks hands even in your peripheral vision Strong tracking No haptic feedback Self-occlusion of hands Limited API
	Cons	<ul style="list-style-type: none"> Tracks hand only in your conical vision Tracks hands even in your peripheral vision Weak in bimanual manipulations Extremely noisy Strong API 	

suggest that Noitom Hi5 had the best performance and provided seamless manipulation and haptic experience both in large and small objects with one-handed or two-handed gestures. The main limitation of Noitom Hi5 is calibration problems and the effects of magnetic fields on the accuracy of motion trackers. The Noitom Hi5 gloves quickly lose calibration in the presence of a small magnetic field from the phone or other devices and require recalibration.

Oculus Quest achieved the second-best performance. Oculus Quest achieved great accuracy and has the ability to track hands in the user's peripheral vision since it has four peripheral cameras mounted on HMD. The main limitation of this device is the lack of haptic feedback. Lastly, Leap Motion achieved the lowest performance because it constantly lost track of the hand positions. Also, Leap Motion can only track the hands in a conical vision, and it loses track if the hands move to the peripheral position.

After an object is grabbed using one of the VM technologies studied in this section, a user needs to place it at the desired location. For AEC applications that use BIM or 3D CAD models, there will be a pre-determined place to where a user should move the virtual object. The next section presents a snap-to-fit function for virtual assembly that will lead to multiple applications in the AEC domain.

Lastly, to quantify the results of this section, the authors have performed each gesture for two minutes (both one and two-handed gestures). The authors have measured the movements captured by each system relevant to their actual position and calculated root mean square error (RMSE). This measurement can quantify the noise associated with each system and provide more insights into each system's robustness ([Table 4](#)). Also, the authors have calculated the number of times that the system lost track of the hands during the course of this test and reported that separately in the last column of [Table 4](#).

4. Snap-to-fit function

The snap-to-fit function acts as a critical intervention for snapping virtually 3D models to a pre-determined location in real-time. An AEC

application of this concept in this paper is the snapping of as-built models (3D scanned models) to as-planned models (BIM/CAD), which can have extended applications for training, inspection/quality assurance. This snap-to-fit function can also be applied to the snapping of as-planned models onto as-planned or as-built models in the same way.

The development of this functionality is challenging since the scanned model with different geometry, meshing, and occlusion rates have to snap into a BIM model accurately. Also, BIM and scanned models have a large number of vertices and faces, which may be challenging for real-time applications. This paper addresses this limitation by introducing a function that can perform snap-to-fit in real-time. This function was tested, validated, and evaluated through an experiment.

4.1. Method

[Fig. 7](#) demonstrates the overall steps of the developed snap-to-fit function. In the first step, the as-built and as-planned models must be segmented. This process splits the mesh into small segments (depending on the selected number of segments), as demonstrated in [Fig. 8](#).

After segmentation, the user grabs the as-built model and try to place it in the as-planned model. During the manual alignment process, the snap-to-fit function calculates a similarity rate, which fixes the as-built model in the position as soon as the similarity rate reaches a certain threshold. Finally, the snap-to-fit function evaluates the scanned model by providing an occlusion rate and a similarity rate. [Fig. 9](#) illustrates a sample scene where a user is grabbing an as-built component and tries to place it in the as-planned position highlighted in green.

The snap-to-fit function operates based on the following mathematical definitions, operations, and steps that compare BIM and scan models segments. In this study a mesh M is defined as a triangulated planar surface that consists of three vertices (V_i, V_j, V_k) . Each vertex V is created from three values showing a 3D coordinate (i.e., x, y, z). Each face F is created by connecting (V_i, V_j, V_k) . The mesh is defined as $M(V, F)$. Consequently, the normal of a face in a mesh \vec{N}_{F_m} is defined as follows:

Table 4

RMSE of palm position for each manipulation system versus each defined gesture (The values in parenthesis are for bimanual manipulation).

Device	Gestures				No. Lost Tracks
	A	B	C	D	
Noitom Hi5	0.215(0.232)	0.393(0.437)	0.186(0.179)	0.210(0.236)	0.251(0.271)
Leap Motion	0.431(0.641)	1.006(1.056)	0.440(0.434)	0.446(0.442)	0.580(0.643)
Oculus Quest	0.576(0.633)	0.437(0.566)	0.173(0.182)	0.238(0.281)	0.356(0.415)

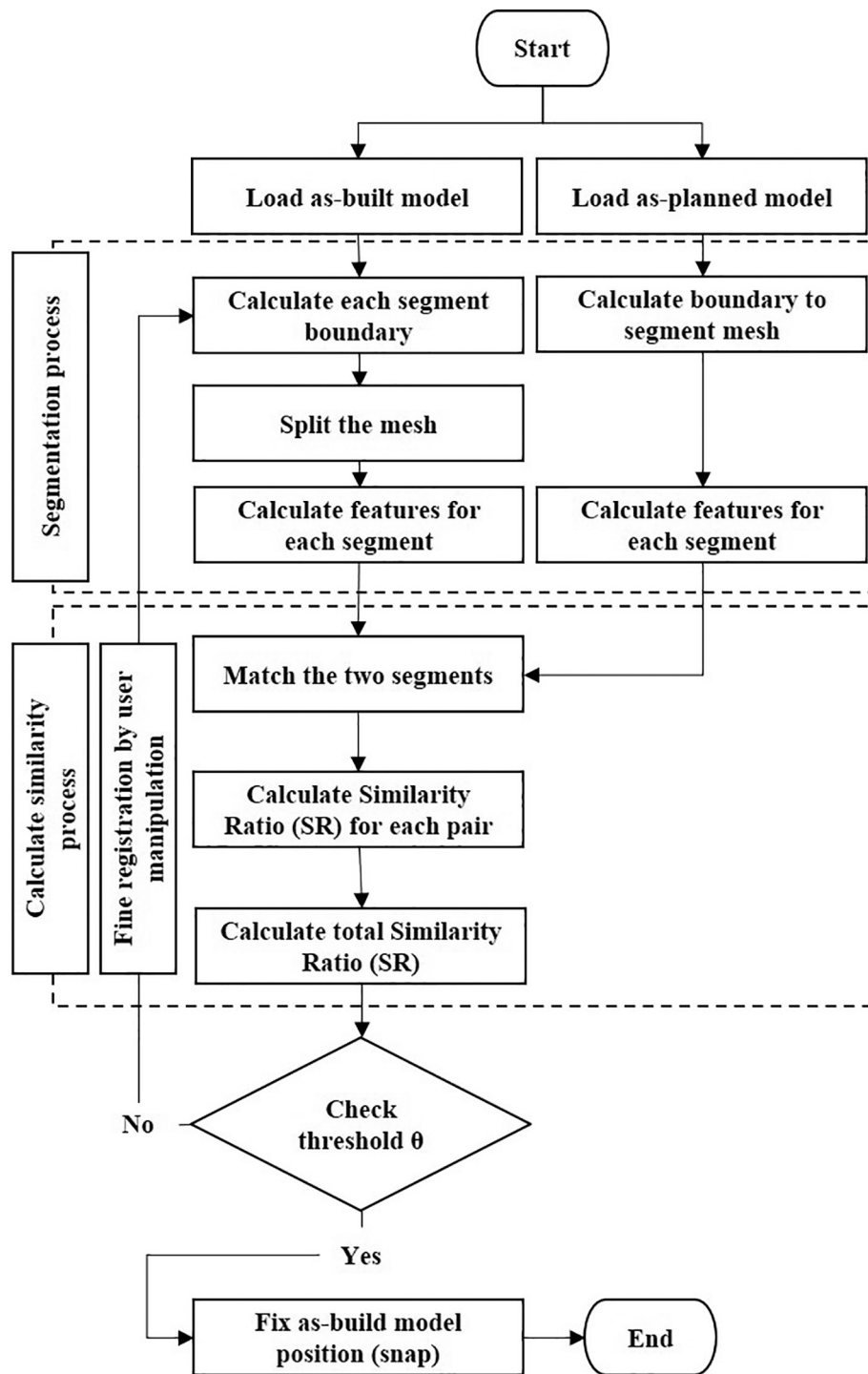


Fig. 7. Snap-to-fit function overview.

$$\forall F_m = \{V_i, V_j, V_k\} \in M(V, F) : \vec{N}_{F_m} = \frac{\left(\vec{V}_i - \vec{V}_j \right) \times \left(\vec{V}_k - \vec{V}_j \right)}{\left| \left(\vec{V}_i - \vec{V}_j \right) \times \left(\vec{V}_k - \vec{V}_j \right) \right|} \quad (1)$$

The highest point (top point) of a mesh or mesh segment M in each direction is defined as follows, where p is (x, y, z) :

$$p^{\max} = \text{Max } (v \in V \text{ in } M(V, F)) \quad (2)$$

Consequently, the lowest point of a mesh or mesh segment M in each direction is defined as follows:

$$p^{\min} = \text{Min } (v \in V \text{ in } M(V, F)) \quad (3)$$

The delta value (the dimension) of a mesh in each direction is defined as follows:

$$\Delta^v = p^{\max} - p^{\min} \quad (4)$$

The upper and lower boundary of each segment is necessary to calculate and useful in the process of segmentation. A segment is defined as follows:

$$\text{seg}(i, j, k) : i, j, k \in \{1, \dots, SC\} \quad (5)$$

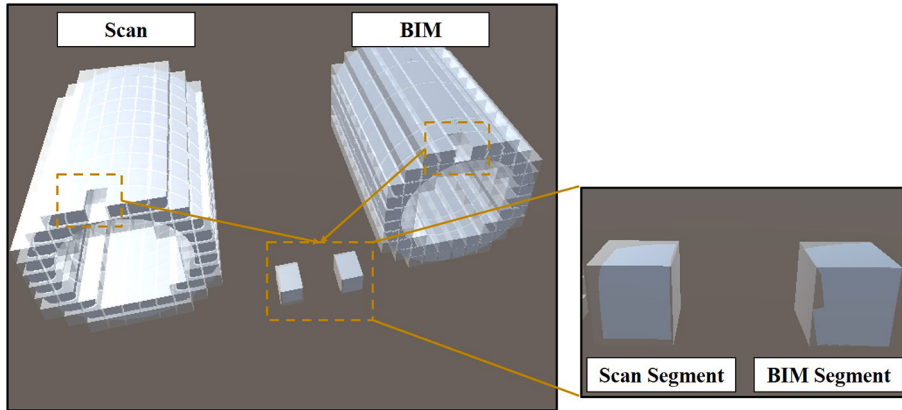


Fig. 8. Segmentation process for BIM and scan models.

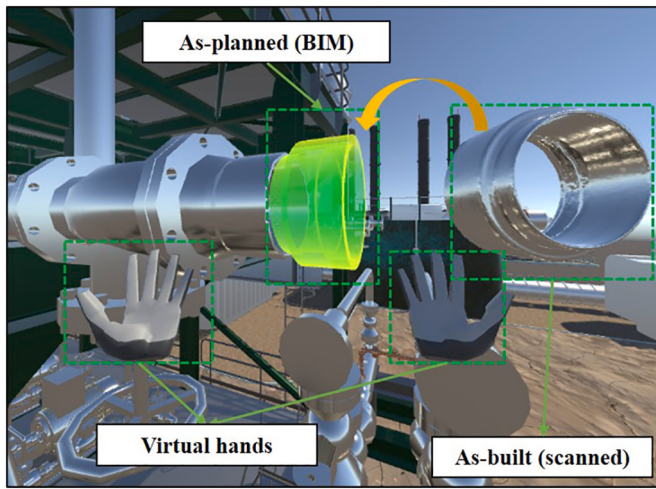


Fig. 9. Segmentation process for BIM and scan models.

Table 5

Features for snap-to-fit function.

Parameters	Formulas
Segment Surface (SS)	$\sum_{F_m=\{V_i, V_j, V_k\} \in F} (V_i - V_j) \cdot (V_k - V_j) / 2$
Segment Dimension (SD)	$X_{M(V,F)}^{\min} - X_{M(V,F)}^{\max}$
Segment Aggregated Normal (SAN)	$\frac{\sum_{F_m=\{V_i, V_j, V_k\} \in F} \vec{N}_{F_m} * (\vec{V}_i - \vec{V}_j)(\vec{V}_k - \vec{V}_j) / 2}{\sum_{F_m=\{V_i, V_j, V_k\} \in F} (\vec{V}_i - \vec{V}_j)(\vec{V}_k - \vec{V}_j) / 2}$

where SC (segment count) is the number of segments in each direction.

Calculation of the boundaries of the segments is useful as these values will be used to split the model (BIM or scan) into the segments. The lower boundary of a mesh segment M in each direction is defined as follows:

$$Bound_{low}^p(seg(i,j,k)) = p^{\min} + \Delta^p * \frac{i - 1}{SC} \quad (6)$$

Similarly, the upper boundary of a mesh segment M in each direction of a segment is defined as follows:

$$Bound_{up}^p(seg(i,j,k)) = p^{\min} + \Delta^p * \frac{i}{SC} \quad (7)$$

To compare the as-built and as-planned segments, the authors defined the three parameters in each segment, as summarized in Table 5.

The first parameter is the surface area of the mesh inside the segment defined as segment surface (SS). The second parameter is the segment dimension (SD), which is defined as the dimensions of the mesh inside the segment. Lastly, the segment aggregated normal (SAN) is defined as a weighted normal vector of the mesh triangles, in which the weights are the area of each triangle.

The following formula (8) is defined to calculate the similarity ratio (SR) between each segment pair. In this formula, the values of each parameter for as-built and as-planned segments are compared and created a ratio which is called SR .

$$\begin{aligned}
 SR(seg_{(i,j,k)}^{M_{Scan}}, seg_{(i,j,k)}^{M_{BIM}}) &= \frac{SS(seg_{(i,j,k)}^{M_{BIM}})}{SS(seg_{(i,j,k)}^{M_{Scan}})} \\
 &\times \prod_{dir=\{x,y,z\}} \frac{SD_{dir}(seg_{(i,j,k)}^{M_{BIM}})}{SD_{dir}(seg_{(i,j,k)}^{M_{Scan}})} \\
 &\times \prod_{dir=\{x,y,z\}} \frac{SAN_{dir}(seg_{(i,j,k)}^{M_{BIM}})}{SAN_{dir}(seg_{(i,j,k)}^{M_{Scan}})} \quad (8)
 \end{aligned}$$

The following formula (9) further expands SR formula for all the segments and to aggregate the total SR from SR between each segment pair.

$$SR(M_{Scan}, M_{BIM}) = \prod_{i,j,k} SR(seg_{(i,j,k)}^{M_{Scan}}, seg_{(i,j,k)}^{M_{BIM}}) \quad (9)$$

Fig. 10 shows a pseudocode that illustrates the process of snap-to-fit function and explains each step of the calculations. This algorithm was implemented in Unity 3D since this 3D engine is able to perform these operations optimally and seamlessly handle user interactions in the VR environment.

4.2. Experimental setup

This section describes an experiment designed to test and validate the performance of snap-to-fit function both in terms of accuracy and time performance. Also, the algorithm's robustness is further discussed by examining it against various occlusions in scanned data (as-built models). Six objects were selected, scanned, and tested in different scenarios.

To make 3D scanned models of the parts, the authors used the Artec Eva [59] and the Artec Leo laser scanners [60]. These hand-held scanners can achieve an accuracy of up to 0.1 mm. Any scanning device/technology that will meet the user's requirement and produce a 3D point cloud can be used for this method. Fig. 11 shows the process of 3D

Algorithm 1: Snap-to-fit algorithm outline

Result: This algorithm segments as-built and as-planned models and matches corresponding segments by user's manipulations

Input: threshold θ ; as-built model; as-planned model; number of segments;

```

/* Initially the models should be segmented */
```

as-built \leftarrow Segmentation(as-built);

as-planned \leftarrow Segmentation(as-planned);

```

/* The algorithm will be executed every i frames to make
sure the algorithm dose not halt the performance of the
program */
```

for (every i frames) **do**

```

SR  $\leftarrow$  Calculate-Similarity(as-built , as-planned);
/* Check if the SR was higher than selected threshold */
if ( $SR > \theta$ ) then
    /* Snap as-build model into as-planned and show the SR
    and OR */
    Snap();
    Vibrate();
end
```

end

Function Segmentation(model: Mesh , Segment Numbers: int) : Mesh[]

```

/* Returns a mesh array (Action 5-7) */
return Mesh[];
end
```

Function Calculate-Similarity(model1: Mesh , model2: Mesh) : float

```

/* A mesh array that contains mesh in each segment */
/* Action 8 */
for (mesh in model1) do
    find-corresponding-mesh-in-model2();
    SR = Formula 8;
end
/* Action 9 */
return combined-similarity-rate;
end
```

Fig. 10. Snap-to-fit function pseudocode.

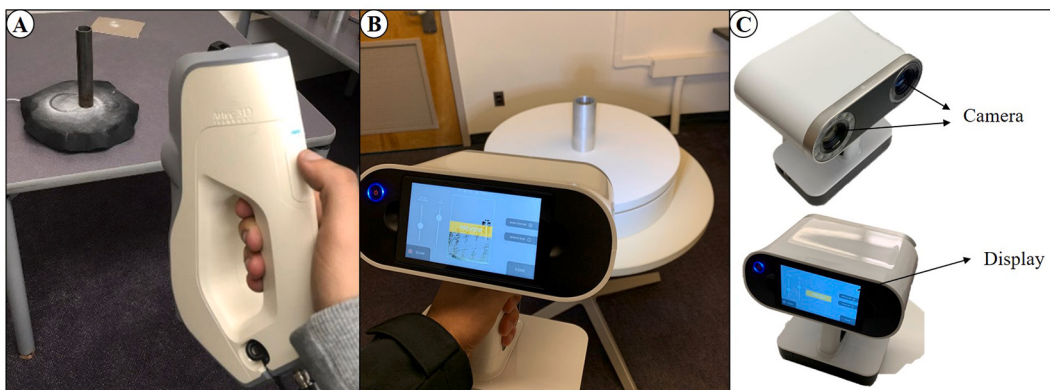


Fig. 11. Scanning objects process; (A) Artec Eva scanning a pipe on a rotary table; (B) Artec Leo scanning a part on a rotary table; (C) Artec Leo overview.

scanning a pipe using the two scanners. The pipe was placed on the rotary table while 3D hand-held scanner stays fixed to generate a 3D scanned model. After scanning the parts, Artec Studio's automated process was used to generate a 3D mesh.

Six objects were selected and scanned to validate the snap-to-fit function. The CAD (computer-aided design) models of the same objects were also acquired. Fig. 12 shows the pictures, scanned models, and BIM models of the six objects. The objects in this section were

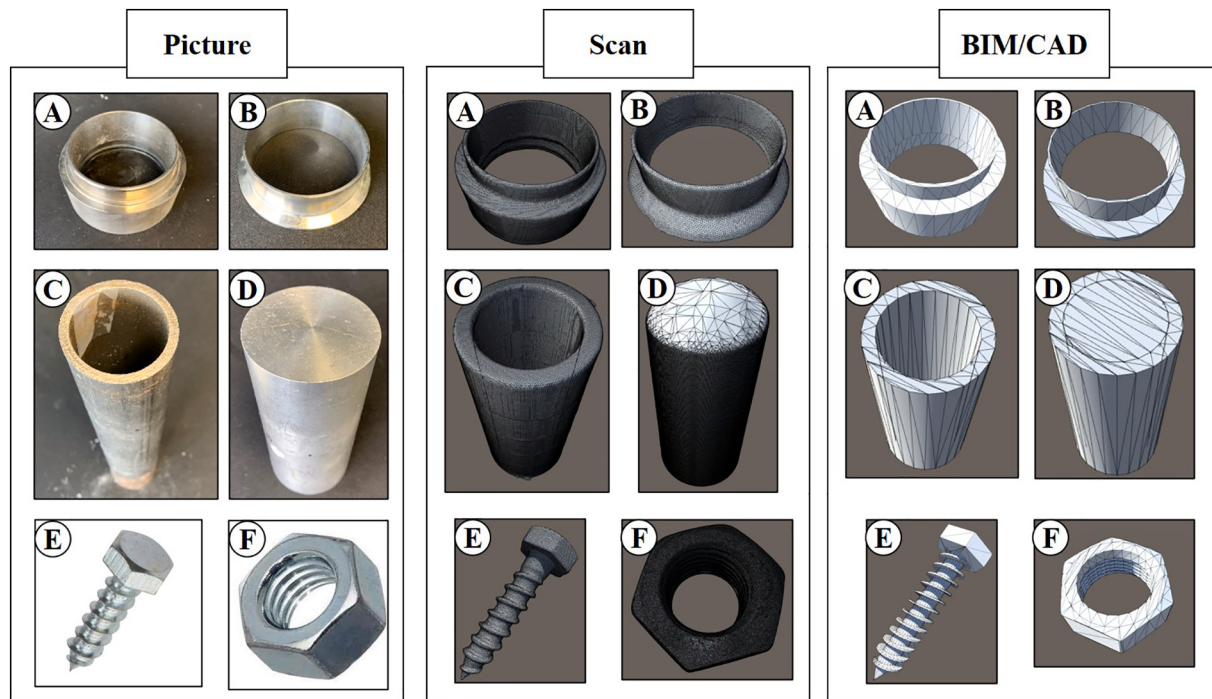


Fig. 12. Scan vs. BIM/CAD model of the used objects.

Table 6

Vertex count of the objects in BIM and scan.

Vertex Count		Object					
		A	B	C	D	E	F
BIM	43,008	18,432	80,802	41,088	36,504	13,260	
Scan	125,742	31,943	82,648	198,402	44,511	446,350	

selected from typically used elements in a piping system as a case study. These objects were selected in a way that they can represent challenges for the snap-to-fit function such as, objects being symmetrical, and they can introduce self-occlusion in the process of scanning.

Table 6 shows the number of vertices for the objects in Fig. 12. The authors used the default number of vertices as initially modeled by the modeling software (3ds Max). The number of vertices for BIM can be changed when exporting the models using BIM/CAD software (3ds Max in this case). Also, the number of vertices for BIM and scan models can be down sampled using an algorithm as introduced later in this section.

Object C in Fig. 12 was manipulated with various degree of occlusions to simulate occluding scenarios that might occur during scanning and show the robustness of the proposed snap-to-fit function. Fig. 13 shows the four occlusion types that were used. The percentage of each scan in Fig. 13 shows the number of presented mesh faces relative to the original scan. This number is later compared to the OR value for validating accuracy.

Fig. 13 shows the segmentation results for 5*5*5, 8*8*8, and 12*12*12 segments (SC in eq. 5). Lastly, Fig. 13 shows various types of missing information from a low range (64% scan meaning only 64% of the vertices from the original scan is presented) to a high range (14% scan meaning only 14% of the vertices from the original scan is presented) and missing interior or part of the object.

Lastly, to validate the time performance of the snap-to-fit function, the accuracy of the snap-to-fit function was tested and validated with various mesh densities. A fast quadratic mesh simplification (FQMS) was used to reduce the mesh density (number of faces/vertices in each mesh) to validate the snap-to-fit for various mesh level of details as the collected visual data size can grow quite large based on the data

collection method used to create 3D models [61,62]. Fig. 14 shows applying FQMS with corresponding percentages for the scanned model of Object A.

4.3. Experimental results

This section summarizes the results of the experiment. HTC Vive VR headset with Noitom Hi5 was used for hand motion tracking. This hardware enables users to interact with virtual objects in an immersive virtual environment (IVE) using their hands. The result of this section was generated using an Intel Core i7-6700K with 64 GB of RAM and a Nvidia GTX 1080 as the graphic card. First, BIM models and scanned models are imported to the IVE. Then, both the VR device and tracker gloves were connected through Unity 3D. In the developed IVE, users can move, rotate, grab, manipulate, and connect virtual elements. This experiment was conducted by the research personnel to measure the performance of the algorithm. The research personnel conducted this experiment for objects A to F in Fig. 12 and tested the time performance as well as the accuracy (SR) of the snap-to-fit function for various scan occlusions, segment counts (SC), and details.

In this IVE, a user can place scanned models in the corresponding and highlighted BIM elements with a snap-to-fit function as shown in Fig. 15. If the SR reaches a selected threshold (0) for the 3D scan and its BIM model, the object will snap into the highlighted area. Otherwise, the part will not snap due to an unacceptable discrepancy, which is an indication that the scanned object is not closely aligned and should not be placed. Since the snap-to-fit function focuses on enhancing the placement process, calculating the accuracy of this function is out of the context of this study. In the context of this study, accuracy is in fact, the output of the

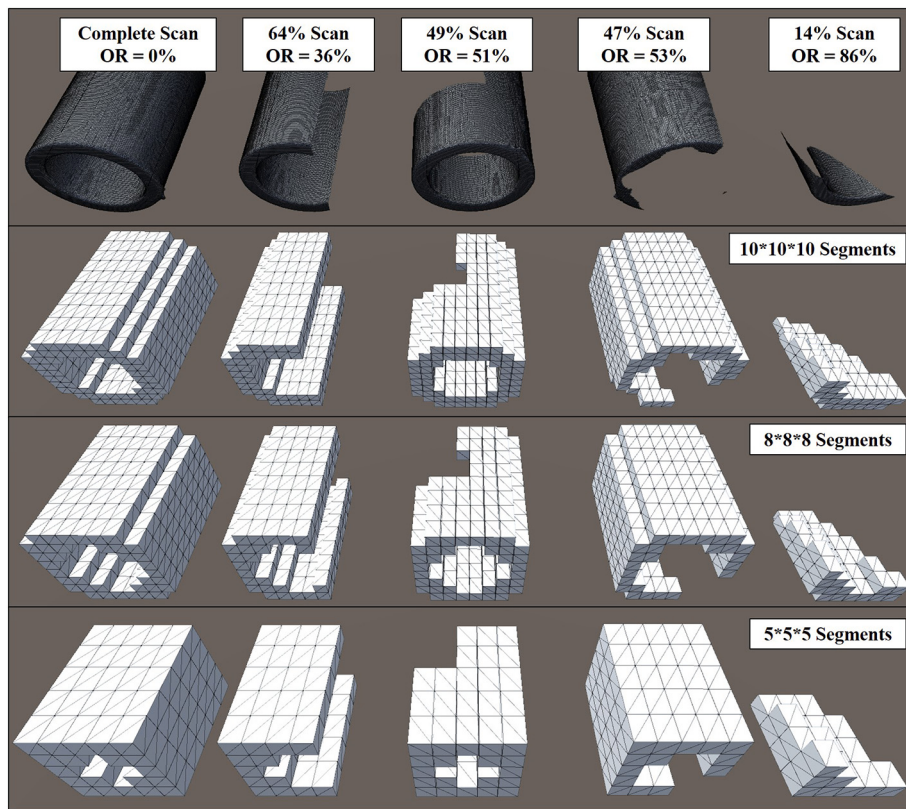


Fig. 13. Segmenting object C for different occlusions level.

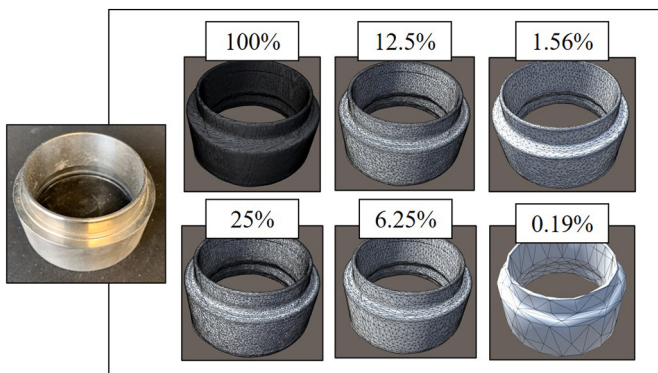


Fig. 14. Resizing scanned mesh using Fast Quadric Mesh Simplification with different level of simplification [63,64].

snap-to-fit function that is defined as SR.

The first section of the experiment validates the robustness and time performance of the snap-to-fit function for various segment counts (SC) and objects. The complete scans (Fig. 12) were aligned with their BIM, and SR between them is computed. With this finding, the appropriate threshold (θ) per segment count can be determined.

Table 7 shows the time performance, and Table 8 shows the SR of the snap-to-fit function. Although the number of points to be processed are the same for different segment counts (SC), increasing segment counts also increased the processing time because the number of calculations increases by an increase in SC. Increasing segment counts also increased SR because the segments get smaller and, therefore, the effect of occlusion and noise in the scanned models is going to be minimal.

The second section of the experiment checks the performance of the snap-to-fit algorithm for occlusion types in Fig. 13 and various levels of

simplification of BIM using FQMS with a $10 \times 10 \times 10$ segment count. Table 9 shows the time performance of the algorithm, and Table 10 shows the SR of the snap-to-fit function. The time performance in Table 9 does not significantly change by variation in BIM detail as changing BIM detail does not affect the number of segments and features in each segment that has to be calculated, whereas, with an increase in OR, the number of non-empty segments can increase and ultimately reduce the required calculations.

A comparison of the time performance of the algorithm and SR shows that SR is robust to the occlusions meaning increasing the OR does not decrease the SR significantly. Also, the time performance of the algorithm and SR has a direct relation with BIM detail. The segmentation process clusters the scan and BIM meshes to deal with occlusions and unscanned areas, e.g., inside a scanned pipe.

The last part of the experiment analyses the SR for various BIM and scan detail levels. In this part of the experiment, 100% BIM detail had the same number of vertices as 100% scan detail. This comparison was conducted to understand whether the difference in the number of vertices in BIM and scans have an impact on SR. Table 11 shows that a decrease in BIM detail can adversely affect SR while a decrease in scan detail does not halt the SR significantly.

Lastly, Fig. 15 shows the actual manipulation of a scanned object using the snap-to-fit function in an IVE. In Fig. 15, the scanned element is hovering the right side, and the position of the BIM element is highlighted by green color. The user grasped the scanned model while the goal is to place the 3D scanned part in the highlighted area. The user moves the part close to the highlighted area, and the scanned model snaps in the highlighted area in green (Fig. 15).

5. Discussion and future works

The first part of this research investigates and compares three main motion tracking methods and hardware (image-based, infrared-based, and magnetic-based). This study found out that magnetic-based

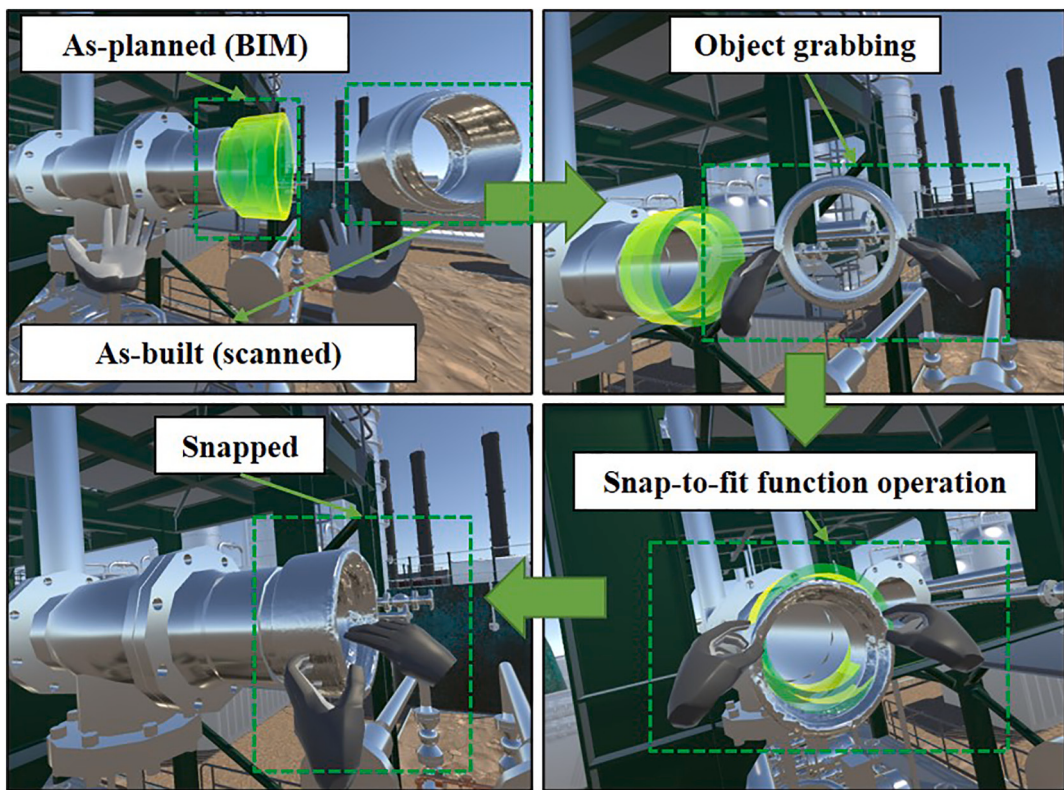


Fig. 15. Simulation of manipulation in VR.

Table 7

Time performance of the snap-to-fit function for various segments counts and objects in seconds.

		Object						
		A	B	C	D	E	F	
Segment Count	(SC)	7*7*7	0.90	0.24	0.74	0.64	0.36	0.90
		8*8*8	1.02	0.38	0.88	0.49	0.46	0.87
		9*9*9	1.29	0.52	1.09	0.65	0.73	0.75
		10*10*10	1.47	0.92	1.64	1.03	1.11	1.36

Table 8

Snap-to-fit function accuracy for various segment counts and objects.

		Object						
		A	B	C	D	E	F	
Segment Count	(SC)	7*7*7	81%	75%	80%	80%	71%	72%
		8*8*8	86%	78%	82%	86%	74%	72%
		9*9*9	86%	82%	81%	89%	77%	76%
		10*10*10	92%	84%	82%	91%	84%	82%

Table 9

Time performance of the snap-to-fit function for object C for different occlusion and BIM details with 10^*10^*10 segment count in seconds.

		BIM Detail			
Occlusion Rate (OR)		8%	13%	25%	100%
0%		1.54	1.68	1.73	1.69
36%		1.47	1.52	1.45	1.71
51%		1.40	1.36	1.33	1.64
53%		1.40	1.38	1.38	1.54
86%		0.87	0.96	0.90	0.94

Table 10

Snap-to-fit function accuracy for object C for different occlusion and BIM details with 10^*10^*10 segment count.

		BIM Detail			
Occlusion Rate (OR)		8%	13%	25%	100%
0%		76%	76%	77%	82%
36%		77%	78%	78%	82%
51%		75%	75%	75%	80%
53%		75%	75%	76%	81%
86%		73%	73%	74%	76%

Table 11

Snap-to-fit function accuracy for object C for various simplification levels of BIM and scan for 10^*10^*10 segment count.

		BIM Detail			
Scan Detail		25%	50%	75%	100%
25%		74.15%	79.57%	81.51%	81.07%
50%		74.79%	78.98%	82.17%	82.02%
75%		74.57%	79.03%	82.50%	82.37%
100%		74.30%	79.04%	82.59%	82.35%

motion tracking is far more accurate compared to the image-based and infrared method. However, the magnetic-based gloves are not stable in the presence of exterior magnetic fields. For example, the presence of metals in the surrounding environment can adversely affect the performance of the motion trackers. The findings outlined in.

Table 3 (pros and cons) suggested that a hybrid approach that combines magnetic-based gloves with image-based motion trackers can potentially solve this deficiency and improve the accuracy of the hand motion trackers in the presence of the magnetic fields. Lastly, the results reported in section 3 are subjective based on the research personnel experience conducting the experiment. The focus of this case study was to see hardware capabilities, revealing advantages and limitations in

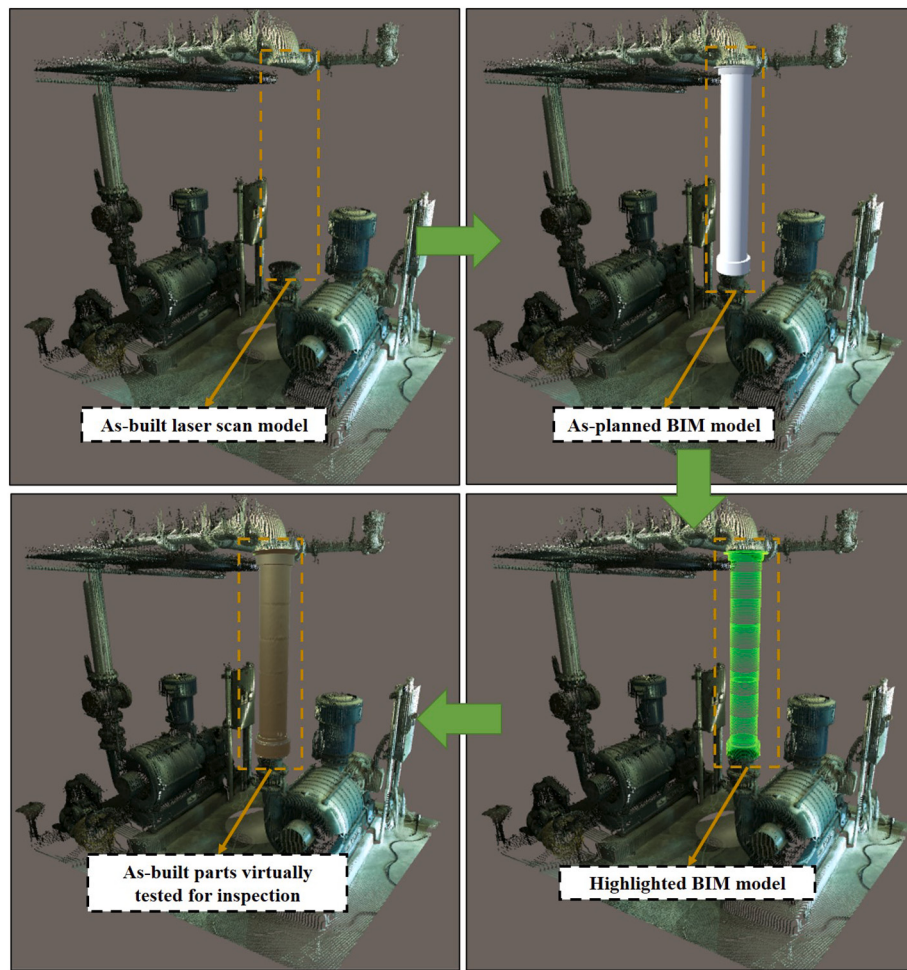


Fig. 16. Simulation of manipulation in VR for virtually bringing and testing the parts before the actual shipment of the parts.

different grabbing scenarios. For detailed experiment to deeply investigate their ability and user-friendliness including how their performance can vary by different users, a structured experiment is necessary and was not scope of this paper.

The second part of this paper solves the placement issue in hand motion tracking systems through the snap-to-fit function. Some of the possible extensions and improvements to this study are documented as follows. The processing time for the snap-to-fit function, as previously reported, can be even longer by increasing the model size and segment count (SC). Therefore, the snap-to-fit function time performance needs to be improved. Potential solutions that can be investigated includes using GPU (graphical processing unit) processing since the snap-to-fit function is inherently a parallel algorithm meaning it contains processes that are independent of each other. Another limitation is that this research does not measure the sense of realism and immersion level of various haptic systems. One potential solution for this limitation is using a systemic experiment that can measure the feelings of human subjects while manipulating objects in section 3. Conducting such experiment can potentially provide more insight on each VM system and help researchers to improve VM hardware by understanding why and how to provide better immersion and sense of realism for the users.

Lastly, the goal of this paper is to introduce a detailed comparison of the VM systems for construction tasks and proposing a snap-to-fit function that can lead to applications in construction and operation and maintenance. For instance, Fig. 16 shows an example of how this research fits in practice and shows the process of bringing elements virtually to the facility (could also be a construction site) and visually inspect and check for compatibility issues before shipping a

prefabricated element. During construction, prefabricated components that arrive on job site will not have compatibility issues after going through this process, similarly, during operation and maintenance, any replacement parts/components (e.g., old steam generator in a power plant) that will arrive at the facility with quality assurance that there will not be any compatibility issue.

6. Conclusion

Over the past few years, AR/VR technologies have received significant popularity in the AEC industry, namely construction safety training, assembly training, construction design review, and inspection. However, there are still numerous research questions to be investigated, such as efficient AR/VR interaction hardware and software. To address this issue and improve the AR/VR interaction, this paper presents a detailed comparison of the state-of-the-art image-based, infrared-based, and magnetic-based VM systems. Also, the second part of this study proposes a novel snap-to-fit function that assesses and performs the compatibility of as-built and as-planned models in real-time. The results of this study show that the magnetic-based VM system outperformed both image-based and infrared-based VM systems. Also, the results demonstrated that a user could automatically check the compatibility of as-built and as-planned models using the snap-to-fit function. Furthermore, the snap-to-fit function was validated in three scenarios to various occlusion types and rates, the number of segment counts, and the as-built and as-planned level of mesh detail. The results are promising, demonstrating the effectiveness and robustness of the proposed snap-to-fit function for VM of the as-built elements and verified the compatibility of the as-built

and as-planned models.

Declaration of Competing Interest

None.

Acknowledgments

This work was partially funded under the Versatile Test Reactor Program of the US Department of Energy (DOE) by Battelle Energy Alliance, LLC (BEA), the Management and Operating Contractor of Idaho National Laboratory (INL) under Contract Number DE-AC07-05ID14517 with DOE and DOE's ARPE-E Program under Award Number DE-AR0001155. The United States Government has a non-exclusive, paid-up, irrevocable, worldwide license to publish and reproduce the published form of this work and allow others to do so, for United States Government purposes. Any opinions, findings, conclusions and/or recommendations expressed in this paper are those of the authors and do not reflect the views of the entities above.

References

- [1] M. Noghabaei, A. Heydarian, V. Balali, K. Han, Trend analysis on adoption of virtual and augmented reality in the architecture, engineering, and construction industry, *Data.* 5 (2020) 26, <https://doi.org/10.3390/data5010026>.
- [2] L.P. Berg, J.M. Vance, Industry use of virtual reality in product design and manufacturing: a survey, *Virtual Reality* 21 (2017) 1–17, <https://doi.org/10.1007/s10055-016-0293-9>.
- [3] S. Choi, K. Jung, S. Do Noh, Virtual reality applications in manufacturing industries: past research, present findings, and future directions, *Concurr. Eng.* 23 (2015) 40–63, <https://doi.org/10.1177/1063293X14568814>.
- [4] S.G. Dacko, Enabling smart retail settings via mobile augmented reality shopping apps, *Technol. Forecast. Soc. Chang.* 124 (2017) 243–256, <https://doi.org/10.1016/J.TECHFORE.2016.09.032>.
- [5] F. Bonetti, G. Warnaby, L. Quinn, Augmented Reality and Virtual Reality in Physical and Online Retailing: A Review, *Synthesis and Research Agenda*, Springer, Cham, 2018, pp. 119–132, https://doi.org/10.1007/978-3-319-64027-3_9.
- [6] H. Zhang, Head-mounted display-based intuitive virtual reality training system for the mining industry, *Int. J. Min. Sci. Technol.* 27 (2017) 717–722, <https://doi.org/10.1016/J.IJMST.2017.05.005>.
- [7] S. Pedram, P. Perez, S. Palmisano, M. Farrelly, Evaluating 360-Virtual Reality for Mining Industry's Safety Training, Springer, Cham, 2017, pp. 555–561, https://doi.org/10.1007/978-3-319-58750-9_77.
- [8] Z. Merchant, E.T. Goetz, L. Cifuentes, W. Keeney-kennicutt, J. Davis, Computers & education effectiveness of virtual reality-based instruction on students' learning outcomes in K-12 and higher education : a meta-analysis, *Comput. Educ.* 70 (2014) 29–40, <https://doi.org/10.1016/j.compedu.2013.07.033>.
- [9] M. Zhang, Z. Zhang, Y. Chang, E. Aziz, S. Esche, C. Chassapis, Recent developments in game-based virtual reality educational laboratories using the microsoft kinect, *International Journal of Emerging Technologies in Learning (IJET)* 13 (2018) 138–159, <https://doi.org/10.3991/ijet.v13i01.7773>.
- [10] S. de Ribaupierre, B. Kapralos, F. Hajli, E. Stroulia, A. Dubrowski, R. Eagleson, Healthcare Training Enhancement through Virtual Reality and Serious Games, *Virtual, Augmented Reality and Serious Games for Healthcare*, 2014, pp. 9–27, https://doi.org/10.1007/978-3-642-54816-1_2.
- [11] X. Wang, P.E.D. Love, M.J. Kim, C.S. Park, C.P. Sing, L. Hou, A conceptual framework for integrating building information modeling with augmented reality, *Autom. Constr.* 34 (2013) 37–44, <https://doi.org/10.1016/j.autcon.2012.10.012>.
- [12] J. Du, Y. Shi, Z. Zou, D. Zhao, CoVR: cloud-based multiuser virtual reality headset system for project communication of remote users, *J. Constr. Eng. Manag.* 144 (2018), 04017109, <https://doi.org/10.1016/ASCECO.1943-7862.0001426>.
- [13] V. Balali, M. Noghabaei, A. Heydarian, K. Han, Improved stakeholder communication and visualizations: real-time interaction and cost estimation within immersive virtual environments, *Construction Research Congress 2018* (2018) 522–530, <https://doi.org/10.1061/9780784481264>.
- [14] V. Balali, A. Zalavadia, A. Heydarian, Real-time interaction and cost estimating within immersive virtual environments, *J. Constr. Eng. Manag.* 146 (2020), 04019098, <https://doi.org/10.1061/ASCECO.1943-7862.0001752>.
- [15] E.Z. Berglund, J.G. Monroe, I. Ahmed, M. Noghabaei, J. Do, J.E. Pesantez, M. A. Khaksar Fasaei, E. Bardaka, K. Han, G.T. Proestos, J. Levis, Smart infrastructure: a vision for the role of the civil engineering profession in smart cities, *Journal of Infrastructure Systems* 26 (2020), <https://doi.org/10.1016/ASCEIS.1943-555X.0000549>.
- [16] F. Biocca, M.R. Levy, T. Kim, M.R. Levy, Communication in the age of virtual reality, *Communication in the Age of Virtual Reality(Routledge Communication Series)*, 2013, pp. 3–14, 1135693579.
- [17] A. Karji, A. Woldesenbet, S. Rokooei, Integration of augmented reality, building information modeling, and image processing in construction management: a content analysis, in: AEI 2017 Resil. Integr. Build. - proc. Archit. Eng. Natl. Conf. 2017, American Society of Civil Engineers (ASCE), 2017, pp. 983–992, <https://doi.org/10.1061/9780784480502.082>.
- [18] X. Li, W. Yi, H. Chi, X. Wang, A.P.C. Chan, Automation in construction a critical review of virtual and augmented reality (VR / AR) applications in construction safety, *Autom. Constr.* 86 (2018) 150–162, <https://doi.org/10.1016/j.autcon.2017.11.003>.
- [19] J. Wolfartsberger, Analyzing the potential of virtual reality for engineering design review, *Autom. Constr.* 104 (2019) 27–37, <https://doi.org/10.1016/j.autcon.2019.03.018>.
- [20] N. Kayhani, H. Taghaddos, M. Noghabaei, U.R. Hermann, Utilization of Virtual Reality Visualizations on Heavy Mobile Crane Planning for Modular Construction, 2018, pp. 1–5, <https://doi.org/10.22260/isarc2018/0170>.
- [21] D. Paes, E. Arantes, J. Irizarry, Immersive environment for improving the understanding of architectural 3D models: comparing user spatial perception between immersive and traditional virtual reality systems, *Autom. Constr.* 84 (2017) 292–303, <https://doi.org/10.1016/j.autcon.2017.09.016>.
- [22] J. Fogarty, J. McCormick, S. El-Tawil, Improving student understanding of complex spatial arrangements with virtual reality, *J. Prof. Issues Eng. Educ. Pract.* 144 (2018), 04017013, [https://doi.org/10.1061/\(ASCE\)EL1943-5541.0000349](https://doi.org/10.1061/(ASCE)EL1943-5541.0000349).
- [23] S. Niu, W. Pan, Y. Zhao, A virtual reality integrated design approach to improving occupancy information integrity for closing the building energy performance gap, *Sustain. Cities Soc.* 27 (2016) 275–286, <https://doi.org/10.1016/j.scs.2016.03.010>.
- [24] L. Hou, X. Wang, L. Bernold, P.E.D. Love, Using animated augmented reality to cognitively guide assembly, *J. Comput. Civ. Eng.* 27 (2013) 439–451, [https://doi.org/10.1061/\(ASCE\)CP.1943-5487.0000184](https://doi.org/10.1061/(ASCE)CP.1943-5487.0000184).
- [25] L. Hou, X. Wang, M. Truijens, Using augmented reality to facilitate piping assembly: an experiment-based evaluation, *J. Comput. Civ. Eng.* 29 (2015), 05014007, [https://doi.org/10.1061/\(ASCE\)CP.1943-5487.0000344](https://doi.org/10.1061/(ASCE)CP.1943-5487.0000344).
- [26] M. Fiorentino, A.E. Uva, M. Gattullo, S. Debernardis, G. Monno, Augmented reality on large screen for interactive maintenance instructions, *Comput. Ind.* 65 (2014) 270–278, <https://doi.org/10.1016/j.compind.2013.11.004>.
- [27] C. Kwiatek, M. Sharif, S. Li, C. Haas, S. Walbridge, Impact of augmented reality and spatial cognition on assembly in construction, *Automation in Construction* 108 (2019), <https://doi.org/10.1016/j.autcon.2019.102935>.
- [28] N. Gavish, T. Gutierrez, S. Webel, J. Rodriguez, M. Peveri, U. Bockholt, F. Tecchia, Evaluating virtual reality and augmented reality training for industrial maintenance and assembly tasks, *Interact. Learn. Environ.* 23 (2015) 778–798, <https://doi.org/10.1080/10494820.2013.815221>.
- [29] M. Murcia-Lopez, A. Steed, A comparison of virtual and physical training transfer of bimanual assembly tasks, *IEEE Trans. Vis. Comput. Graph.* 24 (2018) 1574–1583, <https://doi.org/10.1109/TVCG.2018.2793638>.
- [30] M. Noghabaei, K. Asadi, K. Han, Virtual manipulation in an immersive virtual environment: simulation of virtual assembly, computing in civil engineering: visualization, in: *Information Modeling, and Simulation*, 2019, pp. 95–102, <https://doi.org/10.1061/9780784482421.013>.
- [31] S. Alizadehsalehi, A. Hadavi, J.C. Huang, From BIM to extended reality in AEC industry, *Autom. Constr.* 116 (2020) 103254, <https://doi.org/10.1016/j.autcon.2020.103254>.
- [32] P. Carlson, A. Peters, S.B. Gilbert, J.M. Vance, A. Luse, Virtual training: learning transfer of assembly tasks, *IEEE Trans. Vis. Comput. Graph.* 21 (2015) 770–782, <https://doi.org/10.1109/TVCG.2015.2393871>.
- [33] M. Noghabaei, K. Han, Virtual Manipulation Platform. <https://github.com/mojtaba1995/Virtual-Manipulation-Platform>, 2020. Accessed date: October 9, 2020.
- [34] I. Jeelani, K. Han, A. Albert, Development of Virtual Reality and Stereo-Panoramic Environments for Construction Safety Training, *Engineering, Construction and Architectural Management*, 2020, <https://doi.org/10.1108/ECAM-07-2019-0391>.
- [35] C. Boton, Supporting constructability analysis meetings with immersive virtual reality-based collaborative BIM 4D simulation, *Autom. Constr.* 96 (2018) 1–15, <https://doi.org/10.1016/j.autcon.2018.08.020>.
- [36] H. Taghaddos, A. Mashayekhi, B. Sherafat, Automation of construction quantity take-off: using building information modeling (BIM), *Construction Research Congress 2016* (2016) 2218–2227, <https://doi.org/10.1061/9780784479827.221>.
- [37] X. Li, W. Yi, H.-L. Chi, X. Wang, A.P.C. Chan, A critical review of virtual and augmented reality (VR/AR) applications in construction safety, *Autom. Constr.* 86 (2018) 150–162, <https://doi.org/10.1016/j.autcon.2017.11.003>.
- [38] L. Hou, H.L. Chi, W. Tarnig, J. Choi, K. Panuwatwanich, X. Wang, A framework of innovative learning for skill development in complex operational tasks, *Autom. Constr.* 83 (2017) 29–40, <https://doi.org/10.1016/j.autcon.2017.07.001>.
- [39] B. Bodenheimer, S. Creem-Regehr, J. Stefanucci, E. Shemetova, W.B. Thompson, Prism aftereffects for throwing with a self-avatar in an immersive virtual environment, *Proceedings - IEEE Virtual Reality.* 0 (2017) 141–147, <https://doi.org/10.1109/VR.2017.7892241>.
- [40] M. Fiorentino, R. Radkowski, C. Stritzke, A.E. Uva, G. Monno, Design review of CAD assemblies using bimanual natural interface, *Int. J. Interact. Des. Manuf.* 7 (2013) 249–260, <https://doi.org/10.1007/s12008-012-0179-3>.
- [41] M. Chu, J. Matthews, P.E.D. Love, Integrating mobile building information modelling and augmented reality systems: an experimental study, *Autom. Constr.* 85 (2018) 305–316, <https://doi.org/10.1016/j.autcon.2017.10.032>.
- [42] D.Y. De Moura, A. Sadagic, The effects of stereopsis and immersion on bimanual assembly tasks in a virtual reality system, in: *26th IEEE Conference on Virtual Reality and 3D User Interfaces, VR, 2019*, pp. 286–294, <https://doi.org/10.1109/VR.2019.8798112>.
- [43] M. Kurien, M.K. Kim, M. Kopsida, I. Brilakis, Real-time simulation of construction workers using combined human body and hand tracking for robotic construction

- worker system, *Autom. Constr.* 86 (2018) 125–137, <https://doi.org/10.1016/j.autcon.2017.11.005>.
- [44] J. Czarnowski, A. Dąbrowski, M. Maciąś, J. Główka, J. Wrona, Technology gaps in human-machine interfaces for autonomous construction robots, *Autom. Constr.* 94 (2018) 179–190, <https://doi.org/10.1016/j.autcon.2018.06.014>.
- [45] Y. Fang, Y.K. Cho, F. Druso, J. Seo, Assessment of operator's situation awareness for smart operation of mobile cranes, *Autom. Constr.* 85 (2018) 65–75, <https://doi.org/10.1016/j.autcon.2017.10.007>.
- [46] Q.H. Le, J.W. Lee, S.Y. Yang, Remote control of excavator using head tracking and flexible monitoring method, *Autom. Constr.* 81 (2017) 99–111, <https://doi.org/10.1016/j.autcon.2017.06.015>.
- [47] F. Morosi, M. Rossoni, G. Caruso, Coordinated control paradigm for hydraulic excavator with haptic device, in: *Automation in Construction* 105, 2019, <https://doi.org/10.1016/j.autcon.2019.102848>.
- [48] T. Hilfert, M. König, Low-cost virtual reality environment for engineering and construction, *Visualization in Engineering*. 4 (2016) 2, <https://doi.org/10.1186/s40327-015-0031-5>.
- [49] G. Du, G. Yao, C. Li, P.X. Liu, Natural Human Robot Interface Using Adaptive Tracking System with the Unscented Kalman Filter, in: *IEEE Transactions on Human-Machine Systems*, 2019, <https://doi.org/10.1109/THMS.2019.2947576>.
- [50] J. D'Abbraccio, L. Massari, S. Prasanna, L. Baldini, F. Sorgini, G. Airò Farulla, A. Bulletti, M. Mazzoni, L. Capineri, A. Menciassi, P. Petrovic, E. Palermo, C. Oddo, Haptic glove and platform with gestural control for neuromorphic tactile sensory feedback in medical telepresence, *Sensors*. 19 (2019) 641, <https://doi.org/10.3390/s19030641>.
- [51] V. Getuli, P. Capone, A. Bruttini, S. Isaac, BIM-based immersive virtual reality for construction workspace planning: a safety-oriented approach, *Autom. Constr.* 114 (2020) 103160, <https://doi.org/10.1016/j.autcon.2020.103160>.
- [52] Y. Shi, J. Du, C.R. Ahn, E. Ragan, Impact assessment of reinforced learning methods on construction workers' fall risk behavior using virtual reality, *Autom. Constr.* 104 (2019) 197–214, <https://doi.org/10.1016/j.autcon.2019.04.015>.
- [53] S. Alizadehsalehi, A. Hadavi, J.C. Huang, Virtual reality for design and construction education environment, in: *AEI*, 2019, pp. 193–203, <https://doi.org/10.1061/9780784482261.023>, n.d.
- [54] S. Alizadehsalehi, A. Hadavi, J.C. Huang, BIM/MR-lean construction project delivery management system, in: *2019 IEEE Technology Engineering Management Conference (TEMSCON)*, 2019, pp. 1–6, <https://doi.org/10.1109/TEMSCON2019.8813574>.
- [55] K. Sebastian, T. Ghose, M. Huff, Repeating virtual assembly training facilitates memory for coarse but not fine assembly steps, *J. Comput. Assist. Learn.* 34 (2018) 787–798, <https://doi.org/10.1111/jcal.12285>.
- [56] M. Noghabaei, K. Han, Hazard recognition in an immersive virtual environment: Framework for the simultaneous analysis of visual search and EEG patterns, *Construction Research Congress*, 2020, <https://doi.org/10.1061/9780784482865.099>.
- [57] Noitom, Noitom Hi5 VR Glove. <https://hi5vr手套.com/>, 2020. Accessed date: January 24, 2020.
- [58] L. Motion, Leap Motion Controller. <https://www.ultraleap.com/product/leap-motion-controller/>, 2020. Accessed date: January 24, 2020.
- [59] Artec Eva. <https://www.artec3d.com/portable-3d-scanners/artec-eva>, 2018. Accessed date: February 12, 2018.
- [60] Artec Leo 3D Scanner - The first scanner to offer automatic onboard processing. <https://sourcegraphics.com/3d/scanners/artec/leo/>, 2020. Accessed date: March 2, 2020.
- [61] Fast Quadric Mesh Simplification. <https://github.com/Whinarn/UnityMeshSimplifier>, 2020. Accessed date: August 5, 2020.
- [62] M. Kamari, Y. Ham, Vision-based volumetric measurements via deep learning-based point cloud segmentation for material management in jobsites, *Autom. Constr.* 121 (2021) 103430, <https://doi.org/10.1016/j.autcon.2020.103430>.
- [63] M. Garland, P.S. Heckbert, Simplifying surfaces with color and texture using quadric error metrics, *IEEE Visualization*, 1998, pp. 263–269, <https://doi.org/10.1109/visual.1998.745312>.
- [64] G. Christopher, Healey, 3D Modeling and Parallel Mesh Simplification | Intel® Software. <https://software.intel.com/en-us/articles/3d-modeling-and-parallel-mesh-simplification>, 2015. Accessed date: January 24, 2020.